JOURNAL OF AGRICULTURAL AND FOOD CHEMISTRY

Interactions of Soy Protein Fractions with High-Methoxyl Pectin

MONICA LAM,[†] PAUL PAULSEN,[§] AND MILENA CORREDIG*,[†]

Department of Food Science, University of Guelph, Guelph, Ontario N1G 2W1, Canada, and The Solae Company, St. Louis, Missouri 63110

A protein-binding technique was employed to visualize, using scanning electron microscopy, the soy protein as well as the association between HMP and soy protein fractions. Image analysis indicated that at pH 7.5 and 3.5 soy protein isolate showed a bimodal distribution of sizes with an average [$d(0.5)$] of about 0.05 μm, but at pH 3.8 the proteins formed larger aggregates than at high pH. Addition of HMP at pH 3.8 changed the surface charge of the particles from +20 to −15 mV. A small addition of HMP caused bridging of the pectin between soy protein aggregates and destabilization. With sufficient HMP, the suspensions showed improved stability to precipitation. The microscopy images are the first direct evidence of the interactions between soy proteins with high-methoxyl pectin (HMP).

KEYWORDS: Soy proteins; high-methoxyl pectin; protein−polysaccharide interactions

INTRODUCTION

Pectin is an anionic polysaccharide consisting of a backbone of galacturonic acid partly methylesterified, with branches of arabinose, galactose, and xylose, commonly employed as a stabilizer in protein-based beverages. Due to its great diversity in structure and composition, pectin is characterized by a wide range of functionalities, from emulsifier to gel former or viscosity enhancer (*1, 2*). Pectins can also be used for their ability to interact with proteins at low pH and help stabilize acid dispersions. High-methoxyl pectins (HMP) have a high degree of methylesterification (DE) and have been shown to be particularly efficient in improving the texture and stability of acid milk dispersions (*3, 4*).

The mechanisms leading to the formation of complexes between milk proteins and HMP are well understood (*5, 6*). It has been shown that at pH <5.0 HMP interacts with the positive patches of the protein particle and forms soluble complexes. In acid milk dispersions, HMP adsorbs onto casein particles and a new charged layer forms, which prevents the caseins from aggregating by a combination of electrostatic and steric stabilization (*3–7*).

Whereas a large body of information is available on the interactions between milk proteins and HMP, very little is known on the addition of HMP to acidified soy protein suspensions, although soy proteins are currently employed in many fortified protein beverages. Native soy proteins generally show high solubility at alkaline pH, but their solubility decreases to a minimum in a range of pH from 6.5−3.5 (*8*). The low solubility of soy protein at low pH has limited the use of this ingredient in acid beverages. At low pH soy proteins often form a sediment, and this has significant consequences to the quality of the soy-containing beverages.

The two major components of soy proteins are glycinin (often abbreviated 11S) and β-conglycinin (referred to as 7S). These two globulin proteins represent >85% of the storage proteins in the seed. 11S is a hexameric protein composed of an acidic (about 40 kDa) and a basic (about 20 kDa) polypeptide linked by a single disulfide bond (*9*). 7S (β-conglycinin) is a heterogeneous glycosylated trimeric protein made up of three different subunits: α, α', and β, of 57, 57, and 42 kDa, respectively (*10*). The composition of the various subunits and the ratio between 11S and 7S vary greatly among different soybean varieties. 11S and 7S can be isolated from defatted soy flour by differential isoelectric precipitation (*11, 12*). A better understanding of the differences in the behavior of these two fractions with other ingredients in foods would improve our ability to optimize product formulation and processes.

To better understand the behavior of the various soy protein fractions at low pH, scanning electron microscopy was employed with a protein immobilization technique. A self-assembled monolayer (SAM) of alkane thiols was prepared on a gold-coated carbon planchet. A chemical modification via carbodiimide coupling was then used to covalently bind the soy proteins to the SAM. This technique has been previously employed to study the morphology and size of casein micelles and the structure of caseins in the presence of κ-carrageenan molecules (*13, 14*). The advantage of using this technique is that the SAM acts as a physical barrier to the direct contact of the protein to the solid surface, preventing denaturation or surface-induced spreading of the protein (*14, 15*). More importantly, the protein is covalently bound to the SAM and washing steps can then be performed. This technique was employed to observe the association of HMP with soy protein fractions at pH 3.8.

* Corresponding author (e-mail mcorredi@uoguelph.ca).
[†] University of Guelph.
[§] The Solae Co.

10.1021/jf073375d CCC: $40.75
Published on Web 06/03/2008

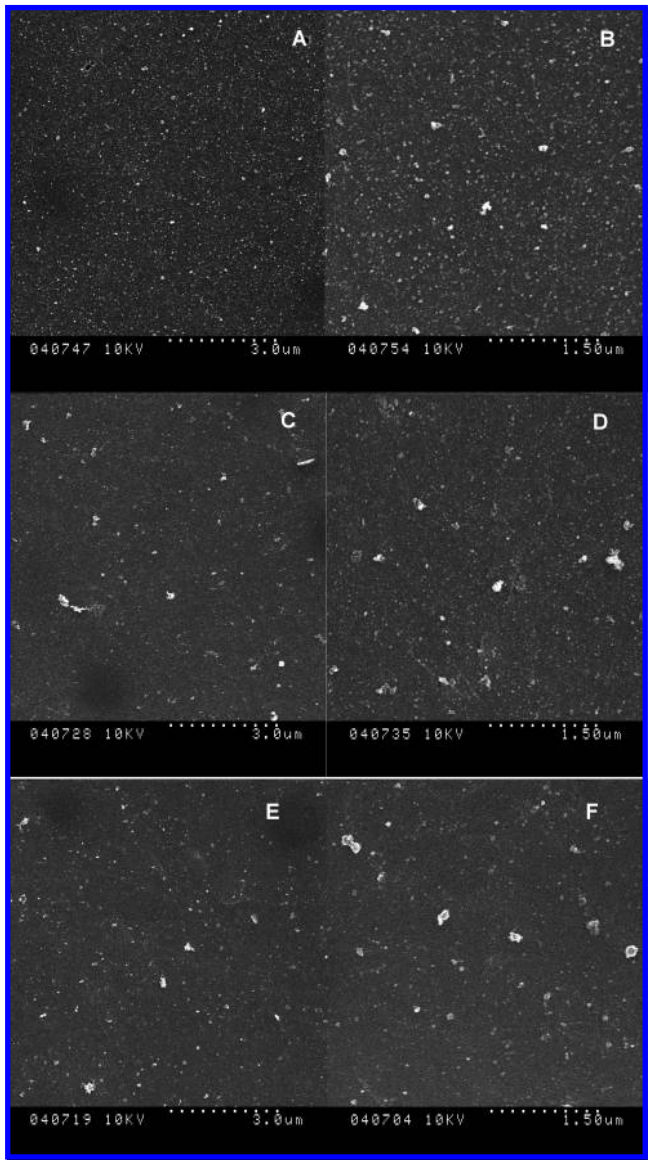

Figure 1. Scanning electron micrographs of SPI (**A**, **B**), 11S (**C**, **D**), and 7S (**E**, **F**) immobilized at pH 7.5. Two different magnifications are shown.

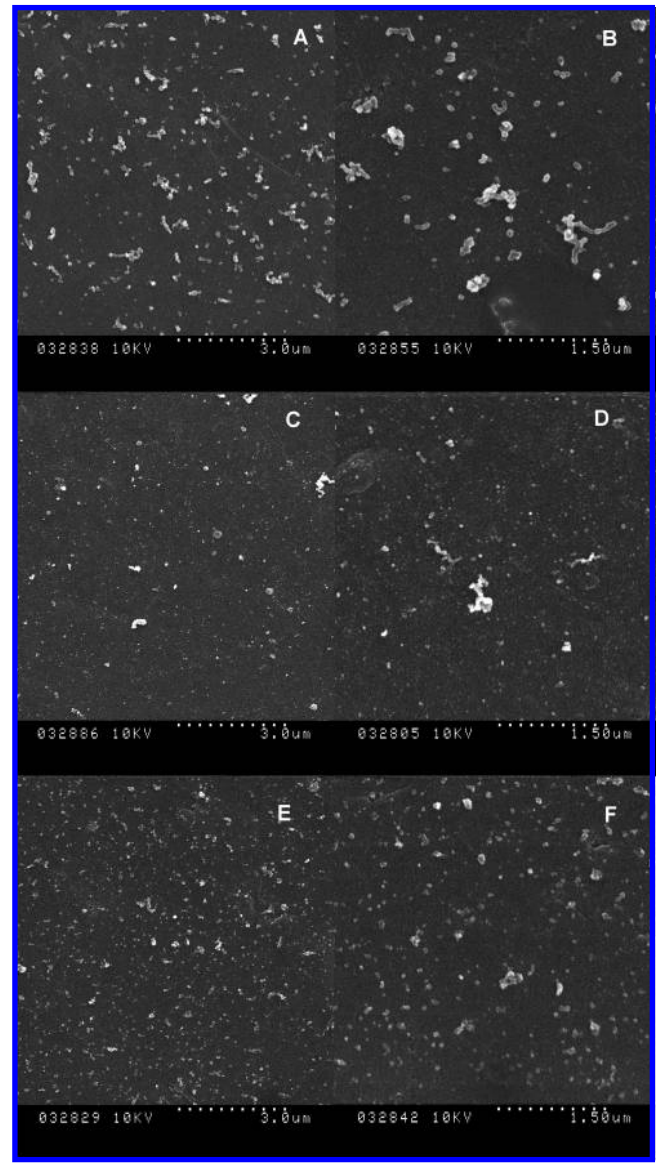

Figure 2. Scanning electron micrographs of SPI (**A**, **B**), 11S (**C**, **D**), and 7S (**E**, **F**) immobilized at pH 3.8. Two different magnifications are shown.

The objective of this work was to document the interactions of HMP with soy protein and its components and to understand how the complexes formed affect the stability of low-pH dispersions.

MATERIALS AND METHODS

Defatted soy flakes (donated by The Solae Co., with a dispersion index of 90) were used to prepare soy protein isolate (SPI) and two fractions rich in 11S or 7S by acid precipitation as previously reported (*8, 12*). The flakes were milled and screened (mesh 60, 35, 20). The soy flour from mesh 60 was used for protein extraction and stored in the refrigerator (4 °C) until needed.

SPI was prepared by dispersing soy flour at 1:10 ratio (w/v) in 100 mM Tris-HCl buffer at pH 8.0. After stirring at room temperature for 1 h, the insoluble fraction was removed by centrifuging at 12000*g* for 30 min at 10 °C. The supernatant was then adjusted to pH 4.8 using 2 M HCl and refrigerated for 2 h at 4 °C. The protein isolate was separated by centrifugation at 12000*g* for 30 min at 10 °C (Beckman Coulter, model J2-21, Fullerton, CA). The protein precipitate was washed with 10 mM sodium acetate at pH 4.8 at 1:8 ratio (w/v) and centrifuged as described above. The soy protein was adjusted to pH 7.0 in ultrapure water and freeze-dried. The amount of protein in the isolate obtained was 94.2% (dry basis) as measured using the Dumas method (using 6.25 factor for protein, approved method 46-30 AACC, 2000).

For extraction of 7S and 11S, soy flour was dispersed at 1:15 ratio (w/v) in ultrapure water, adjusted to pH 7.5 using 1 M NaOH, and stirred for 1.5 h until well solubilized. The insoluble fraction was removed by centrifuging at 12000*g* for 30 min at 20 °C (Beckman Coulter model J2-21). Sodium sulfite was then added to the supernatant to provide 10 mM SO_2 and stirred for 30 min at room temperature. The supernatant was then adjusted to pH 6.4 using 1 N HCl to induce 11S precipitate and stored overnight at 4 °C. The 11S fraction was extracted by centrifuging at 10000*g* for 20 min at 4 °C. A fraction containing both 7S and 11S was removed by adding 0.25 M NaCl to the supernatant and adjusting the pH to 5.0 using 1 N HCl. After stirring for 1 h in an ice bath, the precipitate was separated by centrifugation at 12000*g* for 30 min at 4 °C. The supernatant was then diluted with cold water at 1:1 ratio and adjusted to pH 4.8 using 1 M HCl. The 7S fraction was separated by centrifugation at 10000*g* for 20 min at 4 °C. All of the precipitated fractions were resuspended in ultrapure water and adjusted to pH 7.5. After extensive dialysis against water, the fractions were freeze-dried. The proteins were stored at −20 °C until use.

Stock solutions of 6% protein were prepared by dissolving the isolated fractions in ultrapure water at 65 °C. The solutions were stirred for 10 min and then cooled in an ice bath until they reached room

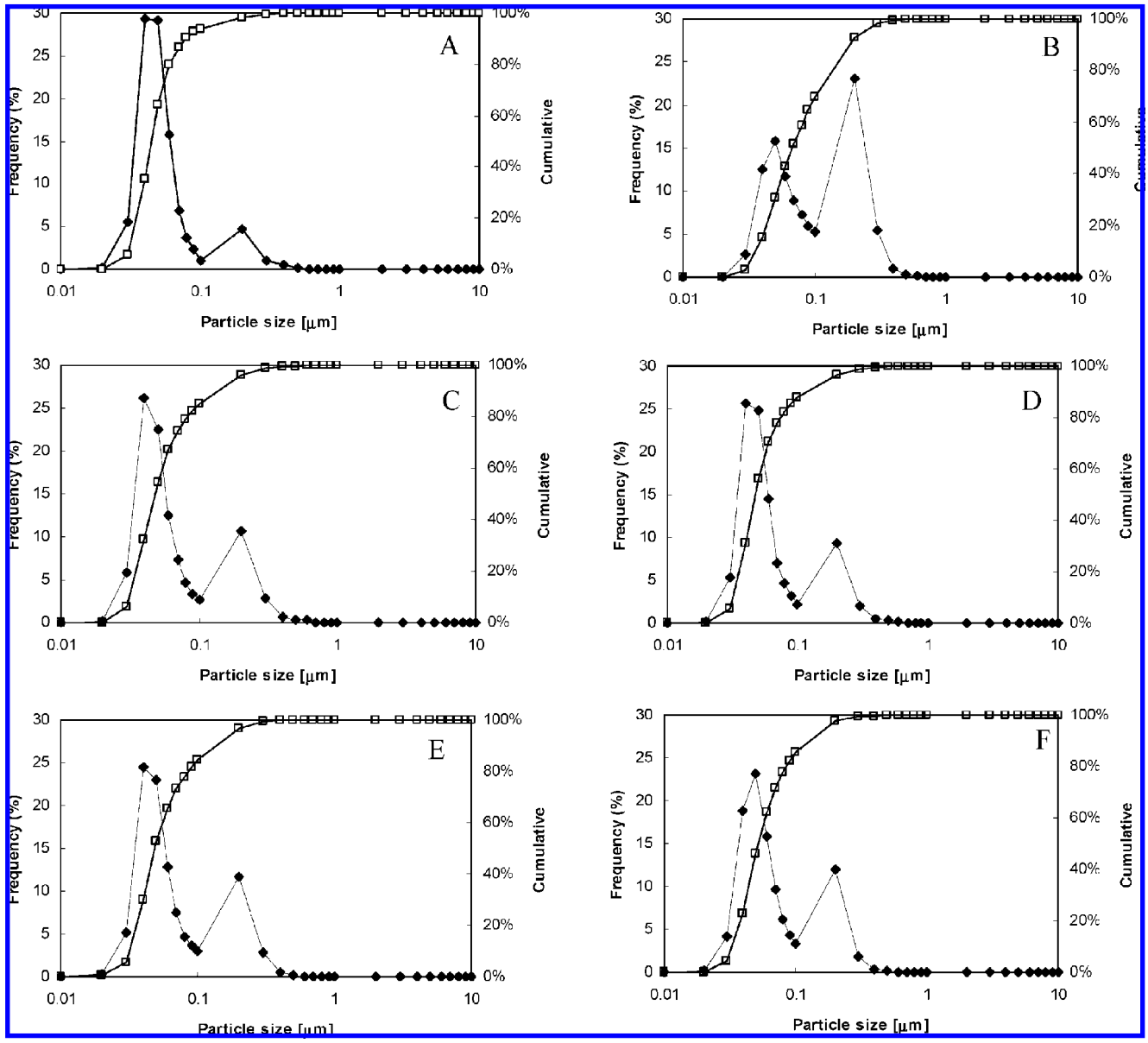

Figure 3. Size distribution (frequency, ◆; and cumulative, □) of the soy protein fractions measured by image analysis for SPI (**A**, **B**), 11S (**C**, **D**), and 7S (**E**, **F**) fractions immobilized at pH 7.5 (**A**, **C**, **E**) or at pH 3.8 (**B**, **D**, **F**).

Table 1. Least-Square Means of the Diameter [*d*(0.5)] Measured by Image Analysis of SPI, 11S, and 7S Soy Protein at pH 3.8 and 7.5

protein	pH	*d*(0.5)[a] (μm)
11S	3.8	0.051 a
11S	7.5	0.051 a
7S	3.8	0.051 a
7S	7.5	0.049 a
SPI	3.8	0.066 b
SPI	7.5	0.049 a

[a] Different letters signify differences at $p < 0.05$.

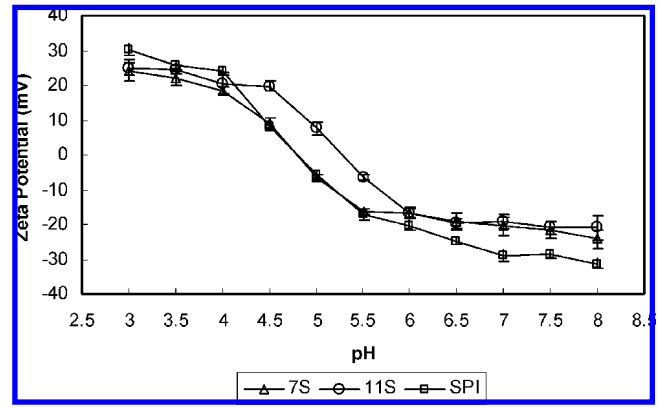

Figure 4. ζ-Potential of the soy protein fractions (SPI, 11S, and 7S) as a function of pH.

temperature. Unstandardized high-methoxyl pectin (HMP) with a degree of esterification (DE) of 71.4 (donated by CPKelco, Denmark) was prepared by dissolving it in ultrapure water at 65 °C and stirring at room temperature for 2 h. Mixtures were prepared to a final concentration of 1.5% protein and various concentrations of HMP (0, 0.10, 0.25, 0.50, and 0.75%). Solutions were adjusted to pH 3.8 using 1 N HCl. Samples containing proteins and pectin were dispersed using a hand-held shear homogenizer (one speed, PowerGen 125, Fisher Sci, Nepean, Canada) for 30 s. Homogenized samples were prepared by passing the mixtures through a high-pressure valve homogenizer (EmulsiFlex-C5, Avestin, Ottawa, Canada) with two passes at 21 MPa. All protein suspensions were stored at 4 °C. All experiments reported were carried out at least in duplicate.

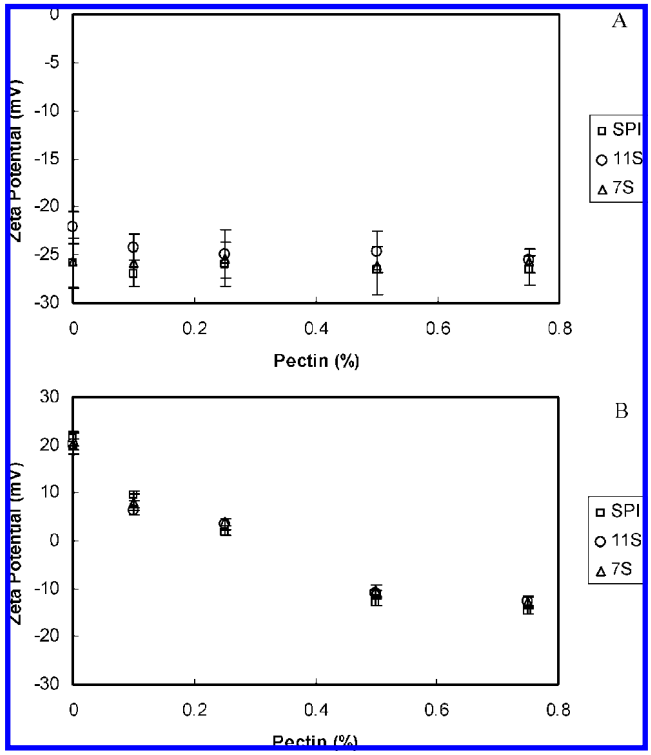

Figure 5. ζ-Potential as a function of HMP added for mixtures containing SPI, 11S, and 7S at pH 7.5 (**A**) and 3.8 (**B**).

The protein composition of the different protein isolates (SPI, 11S, and 7S) was analyzed by SDS−polyacrylamide electrophoresis. SDS-PAGE was also carried out on the protein−HMP suspensions at pH 3.8 to determine if there was any effect of protein type or concentration of HMP on the composition of the soluble phase. SDS-PAGE was performed according to previous papers (*16*) with slight modifications. Twelve percent acrylamide gel with 4% stacking gel in a Bio-Rad mini-protein electrophoresis (Bio-Rad, Missisagua, ON, Canada) was used to separate the protein subunits. A buffer containing 0.75 M Tris-HCl, pH 8.8, and 0.10% SDS was used for the separating gel, and 0.12 M Tris, 0.96 M glycine, and 0.02% SDS, pH 8.3, was used as running buffer. Dried protein samples (6 mg) or sample mixtures (soluble fraction of the protein−HMP mixtures) (500 μL) were mixed with 0.42 mL of buffer containing 5 M urea, 0.20% SDS, 2% mercaptoethanol, and 50 mM Tris at pH 8.0, and then samples were diluted 1:1 with electrophoresis buffer containing 125 mM Tris, 5 M urea, 0.2% SDS, 20% glycerol, and 0.01% bromophenol blue. The solution was heated at 95 °C for 5 min, and 6 μL of samples was loaded. Gels were fixed and stained using Bio-Rad Comassie blue R-250 stain solution (45% methanol, 10% acetic acid, and 0.10% Blue R-250) and destained using 45% methanol, 45% ultrapure water, and 10% acetic acid solution.

Dispersions (10 mL) containing SPI/HMP, 11S/HMP, and 7S/HMP were placed in graduated test tubes and stored under quiescent conditions at 4 °C. The formation of a precipitate was observed over time for up to 2 weeks. Nonhomogenized samples were also analyzed.

The size distributions of SPI/HMP, 11S/HMP, and 7S/HMP dispersions were determined by integrated light scattering using a Mastersizer 2000 (Malvern Instruments, Malvern, U.K.) after homogenization (day 0) and after 3 days and 1 week of storage under quiescent conditions at 4 °C. If a precipitate was formed, only the upper phase was analyzed. Phase-separated samples containing a clear serum on top could not be measured. Mixtures were diluted (approximately 1:300 ratio) in deionized water, and refractive indices of 1.47 and 1.33 were used for the scatterer and the solvent, respectively.

ζ-Potential of the SPI, 11S, and 7S as a function of pH was measured using laser Doppler electrophoresis with a Zetasizer 9000 (Nano ZS, Malvern Instruments). Protein samples (300 μL) were diluted with 9.5 mL of 5 mM $NaNO_3$ adjusted to various pH values in the range from 3 to 8 with 0.1 N HCl or 0.1 N NaOH. Complexes of protein and HMP were also analyzed to determine the ζ-potential at pH 3.8 and 7.2. The samples were diluted in 5 mM $NaNO_3$ at pH 3.8 and 7.2.

Dynamic light scattering (DLS) was used to further characterize the complexes in protein−pectin mixtures at pH 3.8 after the addition of pectinase as previously reported (*17*). The experiments were carried out with a Zetasizer 9000 (Nano ZS, Malvern Instruments) after 1 day of storage of the protein−HMP mixtures. Protein−pectin mixtures (15 μL) were diluted in 3 mL of 0.1 M citrate buffer at pH 3.8 and filtered through a 0.22 μm filter (Whatman, Fisher Scientific, ON, Canada). Appropriate dilutions (3 μL of a solution prepared by adding 10 μL of enzyme in 3 mL of 0.1 M citrate buffer) of pectinase (from *Aspergillus aculeatus*, 9414 u/mL, Sigma, St. Louis, MO) were added to the diluted protein−HMP suspensions to observe the changes of complex sizes every 2 min for up to 40 min (*17*).

Protein immobilization was performed as previously described for milk proteins (*13*), with minor modifications. Carbon planchets were finely polished, washed with detergent, and sonicated for 5 min. The planchets were rinsed with ultrapure water, 95% ethanol, and water again. After air-drying overnight, they were sputter-coated with gold (Emitech K550, Ashford, Kent, U.K.) with a thickness of about 35 nm. Chemisorption of alkane thiols $[CH_3-(CH_2)_{n-1}-SH]$ (11-mercaptoundecanoic acid, 11-MUA) on gold-plated carbon planchets was carried out by reacting the planchets with a 2 mM 11-MUA solution in 100% ethanol for at least 18 h; this formed a self-assembled monolayer. The planchets were rinsed with 95% ethanol and ultrapure water. Protein immobilization was then carried out by covalently linking the free end carboxyl group of the SAM with the amino groups of the soy proteins, placing the planchets in 0.1 M *N*-hydroxysuccinimide (NHS) and 0.4 M *N*-ethyl-*N*-(dimethylaminopropyl)carbodiimide (EDC) for 20 min (*13, 14*). The samples were then rinsed with ultrapure water and placed in either 3% protein solutions or soy protein−HMP suspensions (3% protein and 1.5 or 0.5% HMP) for 1 h. The slides were then rinsed with 10 mM citrate buffer at pH 3.8 or with 10 mM sodium phosphate buffer at pH 7.5, depending on the pH condition of the original samples. Efficient immobilization has been shown to occur at low pH (*14*). By using SAM the soy protein will bind covalently, avoiding conformational changes because of surface adsorption. Note that shrinkage may still occur during sample dehydration. Image analysis (see below) was performed on several micrographs to obtain a size distribution of the soy proteins covalently bound to the SAM.

The SAM technique was employed to reveal interactions between proteins and HMP. The lack of reaction of the HMP was tested by exposing the SAM substrate to a pectin solution. The SAM was also reacted with SPI−HMP mixtures, but also in this case the proteins did not react.

The immobilization of the protein resulted in a covalently bound protein layer that withstood the washing procedure; therefore, the binding of HMP with the protein was tested by reacting a HMP solution to the immobilized soy protein. Planchets with immobilized protein were placed in 0.5% HMP solution for 15 min to allow pectin to interact with the protein attached via the linkers. The samples were then rinsed with 0.1 M citrate buffer at pH 3.8.

All planchets were fixed by placing them in 2% glutaraldehyde solution in either 0.10 M citrate buffer at pH 3.8 or 0.10 M phosphate buffer at pH 7.5, depending on the pH of the original sample, for 30 min. The planchets were washed with the appropriate buffer and subjected to an ethanol dehydration cycle with increasing concentrations of ethanol from 70 to 100% with exchanges every 10 min, with three exchanges at 100% ethanol. The samples were then critical point dried with CO_2. Before analysis, the planchets were sputter-coated with a top layer of about 15 nm of Au. Images were acquired with a scanning electron microscope (Hitachi S-570, Tokyo, Japan) at an acceleration voltage of 10 kV using a Quartz PCI software (Vancouver, BC, Canada).

The particle size distribution of the soy protein samples at pH 7.5 and 3.8 was determined using image analysis software (Image-Pro Plus). Three individual experiments were performed for each treatment. For each set, 10 individual image frames were taken. Each frame contained at least 1000 counts in a range counted with the software. The one parameter used for measurement of particle size is average mean diameter (μm). The average mean diameter measures the average length

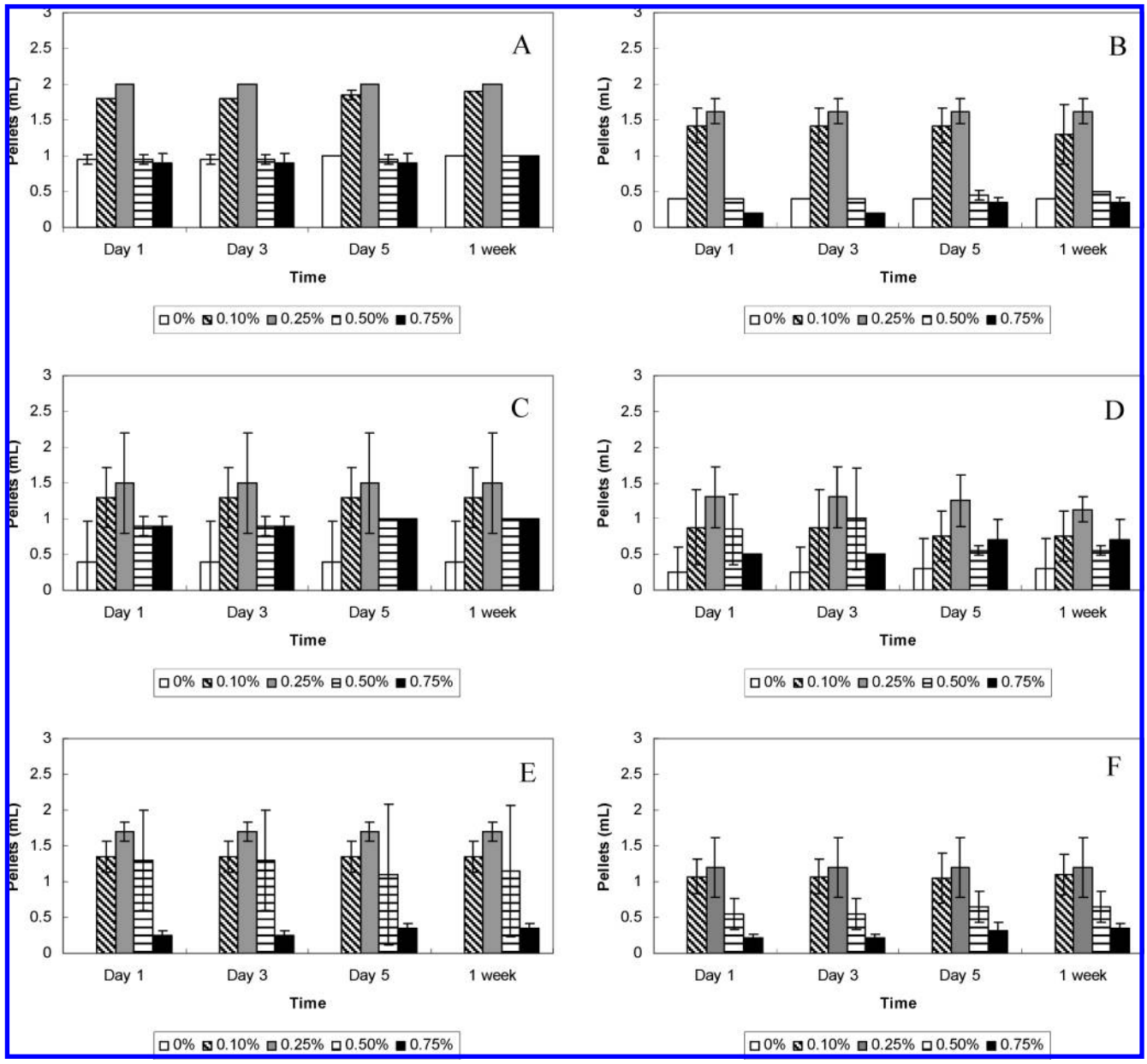

Figure 6. Pellets formed after 1 week of storage at 4 °C. Dispersions contained SPI (**A**, **B**), 11S (**C**, **D**), and 7S (**E**, **F**) and different amounts of HMP [dispersions before (**A**, **C**, **E**) and after homogenization (**B**, **D**, **F**)].

passing through the center point of the particle at every 2° interval. The maximum and minimum diameters of the particle were also measured, but the data are not shown here. Statistical analysis of variance was carried out (SAS, version 8.2) to determine differences in the average size of the proteins depending on the protein fraction or the pH. For this analysis the criterion selected was $d(0.5)$, the midpoint of the cumulative size distribution, where 50% of the particles have a size lower than this value.

RESULTS AND DISCUSSION

To better characterize the soy protein fractions and their behavior at low pH, the soy protein particles from the different fractions were observed by scanning electron microscopy (SEM). The soy proteins were successfully immobilized by carbodiimide chemistry onto gold-coated carbon planchets. To our knowledge, no data are available on the size and microstructure of soy protein particles from soy isolates at both pH 7.5 and 3.8. Using the protein immobilization technique, it was possible to covalently bind the proteins to the carbon support at either pH 7.5 (**Figure 1**) or 3.8 (**Figure 2**). The samples were rinsed of the unbound material with buffer at the corresponding pH and then fixed for SEM. This allowed the determination of the size distribution of the protein particles using image analysis software. **Figure 3** and **Table 1** summarize the results of the size measurements.

SPI at pH 7.5 (**Figure 1A**,**B**) showed a uniform attachment to the carbon planchets, and most proteins showed a spherical structure with a diameter between 50 and 100 nm. It is important to note that the dehydration technique may cause an underestimation of the average size (*13*). Only a few aggregates were observed at this pH. The 11S fraction (**Figure 1C**,**D**) also showed efficient binding to the SAM-covered carbon planchet, and most proteins had a spherical shape; however, this fraction exhibited more aggregates than the SPI fraction, and these aggregates appeared to have elongated structures. At pH 7.5, most protein in the 11S fraction had a diameter of <100 nm. The 7S fraction (**Figure 1E**,**F**) also showed that most proteins

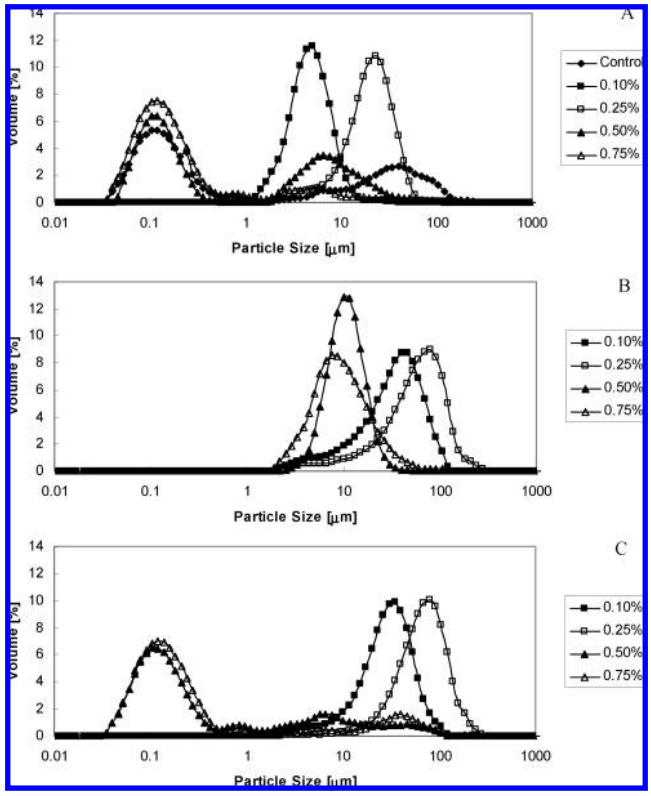

Figure 7. Particle size distribution (measured by integrated light scattering) after homogenization of the dispersions containing SPI (**A**), 11S (**B**), and 7S (**C**), at pH 3.8 as a function of HMP concentration.

had a spherical structure at pH 7.5, and although more aggregates were present than in the SPI fraction, most protein particles were <100 nm.

The presence of a higher number of aggregates in the 11S and 7S fractions at pH 7.5 is probably caused by the history of the protein, as it underwent differential isoelectric precipitation. It is, in fact, possible to hypothesize that the isoelectric precipitation during purification of the soy proteins will affect their aggregation state.

By observing the micrographs of the protein fractions at pH 3.8 (**Figure 2**), it was determined that soy proteins formed large aggregates at pH below the isoelectric point. The binding of the protein to the SAM on the planchet was still efficient as a homogeneous distribution of aggregates was shown in the micrographs. SPI at pH 3.8 showed larger protein particles, with both spherical and elongated type aggregates (**Figure 2A**,**B**). On the other hand, the 11S and 7S fractions seemed to show fewer aggregates compared to SPI (**Figure 2C**−**F**). To be able to better quantify the observations carried out using the protein-binding technique, image analysis was performed, and an average mean diameter and a particle size distribution of the soy proteins in the various isolates at pH 7.5 and 3.8 were calculated (**Figure 3**). All of the isolates at both pH values showed a bimodal particle size distribution with a population of sizes <100 nm and a population of protein aggregates between 200 and 500 nm. For SPI, whereas at pH 7.5 the $d(0.5)$ was 0.049 μm, at pH 3.8, extensive aggregation occurred, and the $d(0.5)$ showed a significant increase to 0.066 μm (**Figure 3** and **Table 1**). 11S and 7S fractions also exhibited an average diameter of about 50 nm at pH 7.5, with a small population of protein particles >200 nm; however, for these fractions, there was no significant difference with pH in the $d(0.5)$ average (**Table 1**). Statistical analysis demonstrated that there was no significant difference between the $d(0.5)$ of SPI, 11S, and 7S at pH 7.5, but there was a significant increase in size for SPI at pH 3.8.

The overall surface charge of the proteins was determined by measuring the ζ-potential as a function of pH for the three different fractions, as shown in **Figure 4**. All protein isolates displayed a negative surface charge at neutral pH with <−20 mV of ζ-potential. The absolute value of ζ-potential started to decrease at pH <5.5 for all fractions. Whereas SPI and 7S showed very similar trends, 11S showed a shift in the isoelectric point to a higher pH and an overall higher positive charge at pH 4.5, compared to SPI and 7S. The point of 0 charge was reached at pH 4.9 for SPI and 7S, whereas in 11S fractions the same point was reached at pH 5.4. At pH 3.8, all protein fractions showed an overall positive ζ-potential with an average at about 20 mV. These results would suggest that at pH 3.8, all of the fractions were stable because of their positive surface charges, which would prevent further aggregation. The results presented in **Figure 4** were in full agreement with previous research reporting similar trends for soy protein isolates of various composition and processing history (*18, 19*).

The values of ζ-potential were also measured on soy−HMP mixtures at pH 7.5 and 3.8 as a function of HMP added (**Figure 5**). The interactions between soy proteins and HMP are electrostatic in nature and depend on the overall charge of the two biopolymers under particular conditions of pH and ionic strength.

At pH 7.5 the protein complexes were negatively charged, as also shown in **Figure 4**, and the overall charge of the mixtures showed no changes with addition of HMP (**Figure 5A**). No differences were also noted between the different protein fractions, and an average ζ-potential of about −25 mV was measured. On the other hand, at pH 3.8 the ζ-potential of soy mixtures was dependent on the amount of HMP added (**Figure 5B**). At this pH all soy protein fractions had an overall positive charge of about +20 mV. The charge of the protein−HMP complexes decreased with increasing amount of HMP (**Figure 5**). In mixtures containing <0.25% HMP, the overall surface charge of the complexes was still positive. At higher concentrations of HMP (>0.50%) the soy protein−HMP complexes reached a plateau value of ζ-potential of about −15 mV. These results suggested that 0.25% of HMP was not sufficient to fully modify the surface charge of the protein complexes and that after reaching a plateau, further addition of negatively charged biopolymer did not cause a decrease in the charge, because charge-repulsion will take place once enough biopolymer is associated with the complexes. No difference was noted in the charge behavior in the presence of HMP for the different protein fractions. These results confirmed that electrostatic interactions play a major role in the formation of soy protein complexes with HMP at pH 3.8.

To determine the stability of the soy isolate−HMP mixtures at pH 3.8, the amount of sediment formed was measured visually for up to a week of storage under quiescent conditions at 4 °C. **Figure 6** illustrates the amount of sediment formed in homogenized and nonhomogenized soy protein−HMP suspensions. In the absence of HMP, protein suspensions containing 11S or SPI showed a small amount of sediment after 1 week of storage. On the other hand, the 7S protein fraction showed no sediment at pH 3.8 in both homogenized and nonhomogenized samples. There were no changes in the stability trends between homogenized and nonhomogenized samples, and homogenization seemed to decrease the amount of sediment recovered after storage. In all three soy isolates−HMP dispersions, the addition

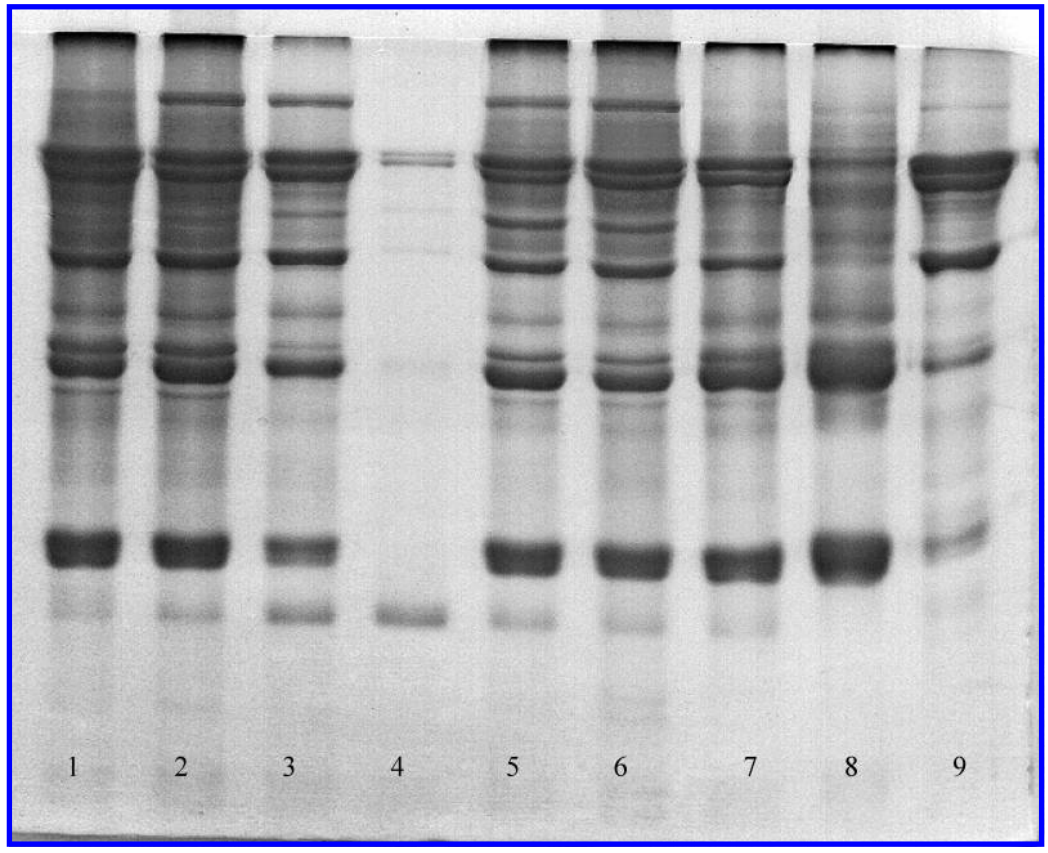

Figure 8. SDS-PAGE of the soluble fractions of SPI dispersions after 1 week of storage. Lanes: 1, SPI with no pectin right after homogenization; 2, SPI with no pectin after 1 week of storage; 3, SPI with 0.1% HMP; 4, SPI with 0.25% HMP; 5, SPI with 0.50% HMP; 6, SPI with 0.75% HMP; 7, SPI fraction; 8, 11S isolate; 9, 7S isolate. Migration direction is from top to bottom.

of 0.10 or 0.25% HMP caused immediate formation of a precipitate with mixing. At these concentrations of HMP, the polysaccharide bridged between protein particles phase separation and complex coacervation, and the large aggregates formed a precipitate. Under these experimental conditions, homogenization did not modify the aggregates and did not decrease significantly the amount of sedimented material during storage. At HMP concentrations $\leq$0.25% measurements of ζ-potential indicated that there were not enough HMP molecules to reach an overall negative charge of the complexes (**Figure 5B**).

The addition of HMP at 0.5 and 0.75% improved the stability of all the dispersions and maintained a turbid appearance. No further changes were noted after 1 week of storage. Homogenization of these dispersions resulted in less sedimented material. Dispersions containing 11S and 0.75% seemed to have more sedimentation than those containing 7S or SPI. This suggested that HMP formed more stable aggregates with SPI or 7S isolates than with 11S protein.

To further characterize the complexes formed in the dispersions, the particle size distribution of the dispersions was determined by diffraction measurements. **Figure 7** summarizes the particle size distribution of SPI, 11S, and 7S dispersions as a function of pectin concentration, measured a few hours after homogenization.

In the absence of HMP, SPI showed a bimodal distribution of sizes with a population of about 0.10 μm of diameter and a small population of large aggregates with a diameter >5 μm (**Figure 7**). After storage, sizes >5 μm will no longer be present in the soluble fraction. Control 11S and 7S suspensions with no pectin added were clear and therefore could not be measured by light scattering. Although all three protein fractions (SPI, 11S, and 7S) were stable at pH 3.8, the results suggested that HMP formed larger bridged complexes with 11S protein particles (**Figure 7B**) than with 7S (**Figure 7C**). Addition of 0.10 or 0.25% HMP caused the formation of large insoluble complexes in all samples. The particle size distribution of the mixtures after homogenization showed sizes of the aggregates between 1 and 80 μm. In all three mixtures, the particle size was bigger in the samples containing 0.25% HMP than those containing 0.1% HMP.

In SPI and 7S dispersions (**Figure 7A**,**C**) HMP added at concentrations >0.5% resulted in a decrease in the particle size distribution. In these dispersions, the addition of 0.5 and 0.75% HMP showed a bimodal distribution of sizes with a diameter around 0.10 μm and small amount of large complexes >8 μm (**Figure 7A**,**C**). In 11S mixtures, the particle size of the complexes was smaller in the 0.5 and 0.75% HMP compared to 0.1 and 0.25%; however, most particles measured showed a diameter >10 μm (**Figure 7B**). It is important to note that for 7S and 11S mixtures, it was visibly noted that the proteins formed complexes with the pectin, as the solutions became turbid after mixing with HMP. The differences in sizes of the complexes formed right after homogenization provided further evidence of the different reactivities of 11S and 7S to HMP at pH 3.8.

After a week of storage at 4 °C, the dispersions containing SPI, 11S, and 7S with 0.1 and 0.25% HMP showed phase separation with a clear supernatant. In all dispersions containing 0.5 and 0.75% HMP, most particles >5 μm were no longer present and only particles between 0.05 and 1 μm were measured in the supernatants.

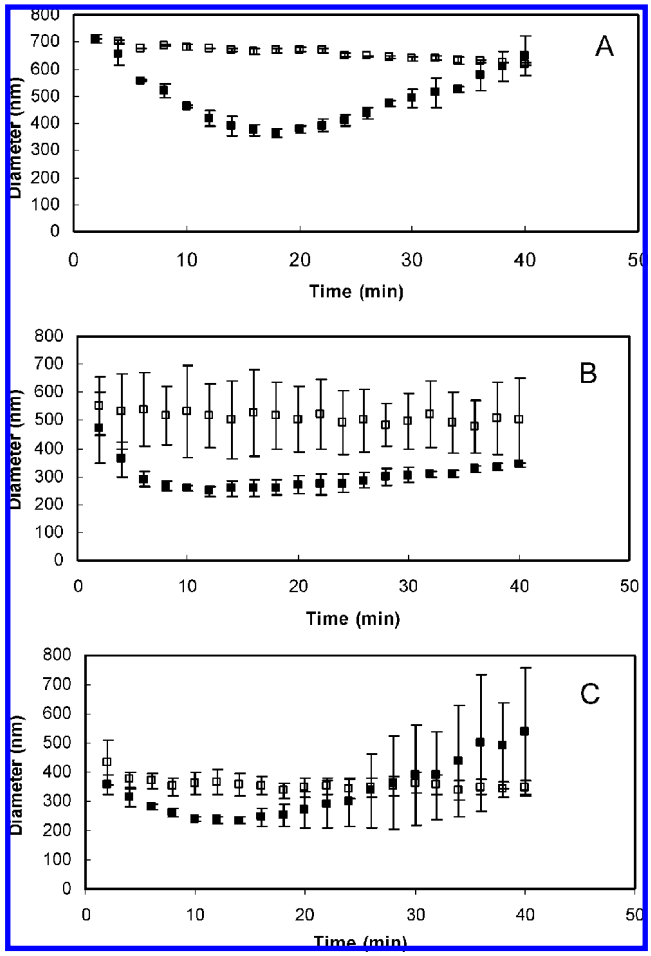

Figure 9. Average apparent diameter measured by dynamic light scattering after the addition of pectinase to diluted suspensions containing 0.75% HMP and SPI (**A**), 11S (**B**), and 7S (**C**). Empty symbols show the size of the complexes with no pectinase added.

SDS-PAGE was carried out on the soluble fractions of the mixtures containing SPI, 11S, and 7S and various concentrations of HMP to determine if soluble complexes were formed preferentially depending on the type of protein present in the dispersion. **Figure 8** shows a representative example of the electrophoretic analyses carried out on the various soluble fractions to obtain information on the polypeptide composition of the soluble phases as a function of HMP added. Although both mixtures containing 0.1 and 0.25% HMP showed a large extent of sedimented material after 1 week of storage, when 0.1% HMP was added to the SPI dispersions, soy proteins were still present in the soluble phase. This confirmed our hypothesis that when small amounts of HMP were added, bridging occurred between the polysaccharide chains and the soy protein particles. A HMP concentration of 0.25% was sufficient to cause the formation of complexes with most of the protein in the mixtures. In the 0.25% HMP−SPI mixture, only a small amount of the α and α′ subunits of 7S were shown in the supernatant. In dispersions containing 0.5 and 0.75% HMP, the protein was again recovered in the supernatant fraction. There was no apparent preferential binding of HMP with any of the soy subunits present. Similar results were shown for the 7S and 11S mixtures (data not shown).

Dynamic light scattering (DLS) measurements were carried out to determine the effect of the addition of pectinase on the apparent hydrodynamic diameter of the complexes formed between soy proteins and HMP. **Figure 9** illustrates the results obtained from 0.75% HMP at pH 3.8. After the dispersions were diluted in citrate buffer at pH 3.8, the average diameter was measured as a function of time after the addition of pectinase. In all of the dispersions it was clearly shown that the addition of pectinase caused a decrease in the apparent diameter of the complexes, and after reaching a minimum, the size would then increase because of protein aggregation. There were obvious differences between the complexes measured from different soy protein dispersions. The largest sizes were measured for the dispersions prepared with 11S fractions. In SPI dispersions (**Figure 9A**) there was a change of about 300 nm during hydrolysis of the pectin by pectinase. Complexes of 11S with 0.75% HMP showed a decrease of about 220 nm (**Figure 9B**), whereas in the 7S complexes with 0.75% HMP, the size change was about 120 nm (**Figure 9C**). It was concluded that a large extent of bridging occurred between HMP and soy protein particles as large differences were shown during the hydrolysis of the HMP molecules in diluted conditions. In addition, the minimum was reached in all samples at about 15 min; however, the 11S−HMP complexes did not seem to show a rapid increase in diameter, unlike SPI and 7S samples. The results from DLS brought further evidence of the formation of complexes between HMP and soy protein at pH 3.8. It could be suggested that these complexes are loose networks of HMP with associated protein particles.

The dispersions containing soy proteins and HMP were also observed using SEM. A protein-binding technique was employed as described above. To confirm that pectin did not bind to the SAM, pectin solutions were also observed with this technique. No pectin was recovered on the carbon support after washing and fixing of the samples. Because the reaction with SAM involves the NH_2 group of the soy protein, pectin will be present on the SAM only if it has an amino group or if interaction with soy proteins has taken place (*13*).

When dispersions containing soy proteins and 0.10% of HMP at pH 3.8 were reacted with the carbon supports with the activated SAM, no pectin, proteins, or soy protein−pectin were observed. It was concluded that in these dispersions, the attachment of the protein particles to the SAM did not take place. Dispersions containing a higher amount of HMP were also tested (0.50%). Also in this case, no pectin, proteins, or soy protein−pectin complexes were observed by SEM. These negative results demonstrated that complexes formed between HMP and soy proteins and that the covalent reaction of the proteins with the SAM was very inefficient. The presence of HMP interfered with the formation of the covalent bond between SAM and proteins. It is possible to hypothesize that there was no accessible site for the proteins for the reaction with SAM.

To confirm the hypothesis that complexes form between the soy proteins and HMP at pH 3.8, the various soy protein fractions at pH 3.8 were first reacted with the SAM and then submerged into pectin solutions at the same pH. The carbon planchets were then rinsed and fixed for SEM observation. All soy fractions showed the formation of complexes with HMP (**Figure 10**). The immobilized SPI, 11S, and 7S proteins showed binding with elongated strands of HMP. It is important to note that although this technique confirmed the association of HMP with soy proteins via electrostatic interactions, it did not show the morphology of the soy protein−HMP complexes, as the washing procedure (with pH 3.8 buffer) and the immobilization of protein result in a very different system from that of the dispersions. In addition, the amount of pectin strands observed on different soy

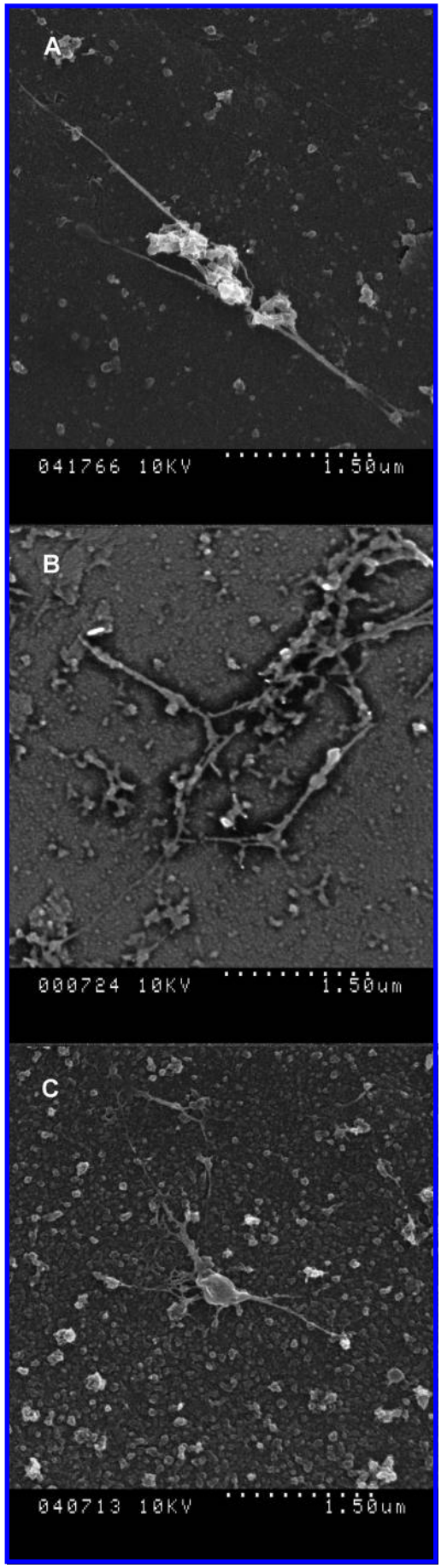

Figure 10. Scanning electron microscopy of cross-linked SPI (**A**), 11S (**B**), and 7S (**C**) at pH 3.8 after reaction with HMP (see Materials and Methods for details).

proteins does not represent the quantity or the preference of binding to the protein, but rather the amount of HMP left on the surface of proteins after extensive washing, fixing, and critical drying.

Electrostatic interactions between soy proteins and HMP play a major role in the formation of stable acid dispersions. At acid pH, HMP formed large complexes with soy protein by bridging with soy protein particles, and HMP prevented protein sedimentation. The different components of soy protein, 11S and 7S, formed different complexes with HMP. This result is relevant to the design of value-added soy protein ingredients.

Values of ζ-potential of the soy protein−HMP dispersions showed a plateau value at the concentrations of HMP that resulted in optimal for complex formation. This could suggest that the ζ-potential could be employed as a tool to optimize the amount of stabilizer needed to form complexes with the protein particles. In addition, immobilization of proteins on a carbon support has been shown successfully in looking at the interactions between soy protein and the HMP at low pH. As far as we know, this work provides for the first time the evidence for the formation of complexes between HMP and soy proteins.

LITERATURE CITED

(1) Willats, W. G. T.; Knox, P. J.; Mikkelsen, J. D. Pectin: new insights into an old polymer are starting to gel. *Trends Food Sci. Technol.* **2006**, *17*, 97–104.

(2) Williams, P. A.; Sayers, C.; Viebke, C.; Senan, C.; Mazoyer, J.; Boulenguer, P. Elucidation of the emulsification properties of sugar beet pectin. *J. Agric. Food Chem.* **2005**, *53*, 3592–3597.

(3) Laurent, M. A.; Boulenguer, P. Stabilization mechanism of acid dairy drinks (ADD) induced by pectin. *Food Hydrocolloids* **2003**, *17*, 445–454.

(4) Nakamura, A.; Yoshida, R.; Maeda, H.; Corredig, M. The stabilizing behavior of soybean soluble polysaccharide and pectin in acidified milk beverages. *Int. Dairy J.* **2006**, *16*, 361–369.

(5) Kazmierski, M.; Wicker, L. W.; Corredig, M. Interactions of β-lactoglobulin and high-methoxyl pectins in acidified systems. *J. Food Sci.* **2003**, *68*, 1673–1679.

(6) Maroziene, A.; de Kruif, K. G. Interactions of pectin and casein micelles. *Food Hydrocolloids* **2000**, *14*, 391–394.

(7) Tromp, R. H.; de Kruif, C. G.; van Eijk, M.; Rolin, C. On the mechanism of stabilization of acidified milk drinks by pectin. *Food Hydrocolloids* **2004**, *18*, 562–572.

(8) Renkema, J.; van Vliet, T. Heat-induced gel formation by soy proteins at neutral pH. *J. Agric. Food Chem.* **2002**, *50*, 1569–1573.

(9) Liu, K. *Soybeans: Chemistry, Technology and Utilization*; International Thomson Publishing: Florence, KY, 1997.

(10) Thanh, V. H.; Shibasaki, K. β-Conglycinin from soybean proteins. *Biochim. Biophys. Acta* **1977**, *439*, 326–338.

(11) Thanh, V. H.; Shibasaki, K. Major proteins of soybean seeds. A straightforward frationation and their characterization. *J. Agric. Food Chem.* **1976**, *24*, 1117–1121.

(12) Nagano, T.; Hirotsuka, M.; Mori, H.; Kohyama, K.; Nishinari, K. Dynamic viscoelastic study on the gelation of 7S globulin from soybean. *J. Agric. Food Chem.* **1992**, *40*, 941–922.

(13) Martin, A.; Goff, D.; Smith, A.; Dalgleish, D. Immobilization of casein micelles for probing their structure and interactions with polysaccharides using scanning electron microscopy (SEM). *Food Hydrocolloids* **2006**, *20*, 817–824.

(14) Uricanu, V. I.; Duits, H. G.; Mellema, J. Hierachical networks of casein proteins: an elasticity based on atomic force microscopy. *Langmuir* **2004**, *20*, 5079–5090.

(15) Wadu-Mesthrige, K. A.; Nabil, A.; Liu, G.-Y. Immobilization of proteins on self-assembled monolayers. *Scanning* **2000**, *22*, 380–388.

(16) Yagasaki, K.; Takai, T.; Sakai, M.; Kitamura, K. Biochemical characterization of soybean protein consisting of different subunits of glycinin. *J. Agric. Food Chem.* **1997**, *45*, 656–666.

(17) Nakamura, A.; Takahashi, T.; Ryuji, Y.; Maeda, M.; Corredig, M. Emulsifying properties of soybean soluble polysaccharide. *Food Hydrocolloids* **2004**, *18*, 795–803.

(18) Lakemond, C.; Jongh, H.; Hessing, M.; Gruppen, H.; Voragen, A. Soy glycinin: influence of pH and ionic strength on solubility and molecular structure at ambient temperature. *J. Agric. Food Chem.* **2000**, *48*, 1985–1990.

(19) Malhotra, A.; Coupland, J. N. The effect of surfactants on the solubility, zeta potential and viscosity of soy protein isolates. *Food Hydrocolloids* **2004**, *18*, 101–108.

Received for review November 19, 2007. Revised manuscript received March 10, 2008. Accepted March 19, 2008. Financial support from the Solae Co. and the Natural Sciences and Engineering Council of Canada is gratefully acknowledged.

JF073375D